



Nanostructured MgH₂ prepared by cold rolling and cold forging

D.R. Leiva^a, R. Floriano^a, J. Huot^b, A.M. Jorge^a, C. Bolfarini^a, C.S. Kiminami^a, T.T. Ishikawa^a, W.J. Botta^{a,*}

^a Departamento de Engenharia de Materiais, Universidade Federal de São Carlos, Rod. Washington Luiz, km 235, 13565-905 São Carlos, SP, Brazil

^b Institut de Recherche sur l'Hydrogène, Université du Québec à Trois-Rivières 3351, Boulevard des Forges, C.P. 500, Trois-Rivières (Québec) G9A 5H7, Canada

ARTICLE INFO

Article history:

Received 1 September 2010

Received in revised form 10 January 2011

Accepted 14 January 2011

Available online 22 January 2011

Keywords:

Metal hydrides

Cold work

Nanostructured materials

Hydrogen storage

ABSTRACT

Magnesium is a promising material for solid state hydrogen storage, since it has low cost and its hydride can store reversibly up to 7.6 wt.% of hydrogen. Fast H-sorption kinetics at around 300 °C can be achieved after processing Mg-based mixtures by high energy ball milling (HEBM), which produces nanostructured composite powders. Severe plastic deformation (SPD) processing techniques are being explored as an alternative to HEBM in order to obtain more air-resistant materials and to reduce the time and energy required for processing. In this paper, MgH₂ and MgH₂-Fe mixtures were severely mechanically processed by extensive cold forging (CF) and cold rolling (CR). A very significant grain refinement (up to 10 nm) was achieved, which is comparable to the values typically obtained after processing by HEBM. Enhanced H-sorption properties were observed for these mechanically processed MgH₂-based nanocomposites in comparison with commercial magnesium hydride. The obtained compacts after CR and CF presents a much lower specific surface area than the ball-milled powders and therefore show higher air-resistance. These results are promising from the point of view of applications since it reveals the potential of the use of low cost mechanical processing routes to produce Mg-based nanomaterials for hydrogen storage.

© 2011 Elsevier B.V. All rights reserved.

1. Introduction

Hydrogen is considered the energy carrier of the future since it presents the highest energetic content among the chemical fuels and the main byproduct of its oxidation is water. Solid state hydrogen storage using metal hydrides is a safer and more effective storing alternative than the use of liquid hydrogen at cryogenic temperatures or gas under high pressures.

Among the metal hydrides, MgH₂ presents the highest gravimetric capacity of 7.6 wt.%. Besides this, magnesium is an abundant cheap metal. The main drawbacks for the application of conventional microcrystalline Mg powder for hydrogen storage applications are the high temperatures needed for H-sorption (>400 °C) and the slow kinetics involved in these processes.

High energy ball milling (HEBM) techniques have been employed to produce MgH₂-based nanocomposite powders containing different types of additives, as for example, transition metals [1], transition metal oxides [2] or fluorides [3]. These materials can present very fast H-sorption kinetics at 300 °C or lower temperatures, taking only a few minutes to achieve complete absorption or desorption reactions.

These improvements are mainly related to the following three effects: (i) the nanocrystalline structure of the matrix, which favors hydrogen diffusion with fast kinetics, (ii) the so-called 'catalytic action' of the additives, which are very finely dispersed in the powders, and (iii) to the very high specific area of the material [4]. However, HEBM is a very intensive time and energy consuming technique. Furthermore, the ball-milled Mg-based powders are usually very reactive in air, and therefore must be manipulated under Ar atmosphere.

Severe plastic deformation (SPD) techniques have been studied as alternative low cost processing routes for Mg alloys for hydrogen storage, aiming to develop more air-resistant materials, with lower specific surface area, but still with attractive H-sorption kinetics. Preparation of Mg-based alloys or composites for hydrogen storage by SPD was first introduced in [5], and since then relevant results appear in the literature [6–8].

However, despite the interest in SPD processing, expressive grain refinement of Mg, which is important for hydrogen storage applications, is difficult to attain due to limited number of slip and twinning systems; therefore, contrary to structures such as fcc which contain a large number of available slip systems, grain refinement in Mg due to equal-channel angular pressing (ECAP) is strongly dependent on the thermally activated recovery processes, and therefore on the processing temperature [9].

Recently, we have studied the hydrogen sorption properties after ECAP of commercial Mg alloys [10] and after consolidation

* Corresponding author. Tel.: +55 16 33518553; fax: +55 16 33615404.
E-mail address: wjbotta@ufscar.br (W.J. Botta).

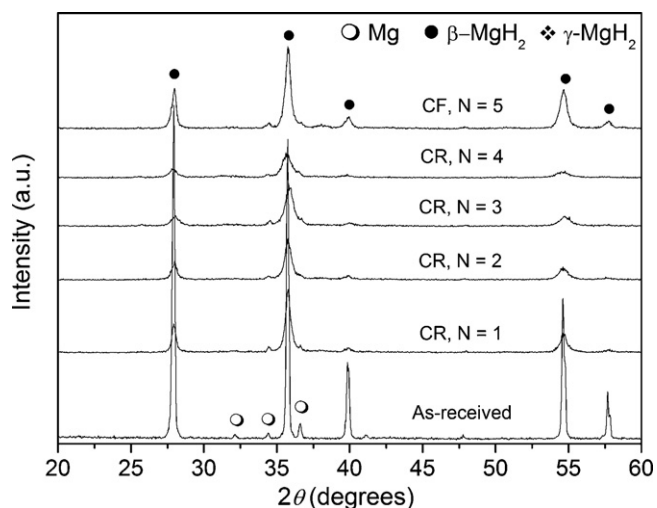


Fig. 1. XRD patterns of MgH_2 after different number of CR and CF passes, as indicated.

by high-pressure torsion (HPT) of Mg , MgH_2 and MgH_2 -Fe mixtures [11]. In the present paper, we detail the first results of the application of extensive cold rolling (CR) and cold forging (CF) to the processing of MgH_2 . The obtained results concerning grain-refinement, H-sorption properties and air-resistance are then compared with powders obtained by HEBM.

2. Experimental

MgH_2 powders (Alfa Aesar, 98%) and MgH_2 -5 at.% Fe mixtures (Fe: Alfa Aesar, 99.99%, previously ball-milled) encapsulated in stainless steel tubes or confined between stainless steel plates were processed by CR and CF.

Forging was carried out by dropping a 30 kg hammer five times from a height of 1.50 m onto the sample. Rolling was performed in a duo-reversible FENN rolling mill, applying up to four passes with 75% of reduction in each pass.

A detailed microstructural characterization of the samples was carried out by X-ray diffraction (XRD), scanning and transmission electron microscopy (SEM and TEM). XRD patterns were obtained using monochromatic $\text{Cu K}\alpha$ radiation with an angular pass of 0.032° , in a Rigaku diffractometer equipped with a C-monochromator operating at 40 kV and 40 mA. The XRD patterns were also used to evaluate the mean crystallite size through Scherrer analysis [12].

SEM images were obtained in a Philips XL-30-FEG microscope. The cold rolled and cold forged compacts were examined by TEM in a FEI TECNAI G2 F20 200 kV microscope.

The H-sorption properties after the first desorption were evaluated in a Sievert type apparatus, using samples with mass of around 100 mg. The hydrogen desorption behaviour of selected samples was investigated by differential scanning calorimetry (DSC) coupled with mass spectrometry (MS), performed in a NETZSCH assembly (STA 449C and QMS 403C). In this case samples with mass of around 10 mg were used. The measurements were performed with the heating rate of $10^\circ\text{C}/\text{min}$.

3. Results and discussion

Fig. 1 shows the XRD patterns of the deformed MgH_2 as a function of number of CR or CF passes. In both cases, the intensity of the diffraction peaks decreases and the peaks become broader with the increase in the number of CR passes or after CF processing. The peak broadening can be attributed to a reduction in crystallite size, which was estimated by Scherrer analysis to be in the range of 10 nm after 4 passes of CR and 26 nm after processing by CF (5 passes). As expected, the average crystallite size of the as-received MgH_2 is much higher than 100 nm and could not be estimated using Scherrer analysis [12].

In the CR samples, a small amount of the high-pressure γ - MgH_2 phase could be identified in addition to the β - MgH_2 phase (Fig. 2). This result shows the ability of CR to produce metastable phases, in a similar way to HEBM [13]. This observation also suggests that CR is more efficient than CF in increasing the free energy of the

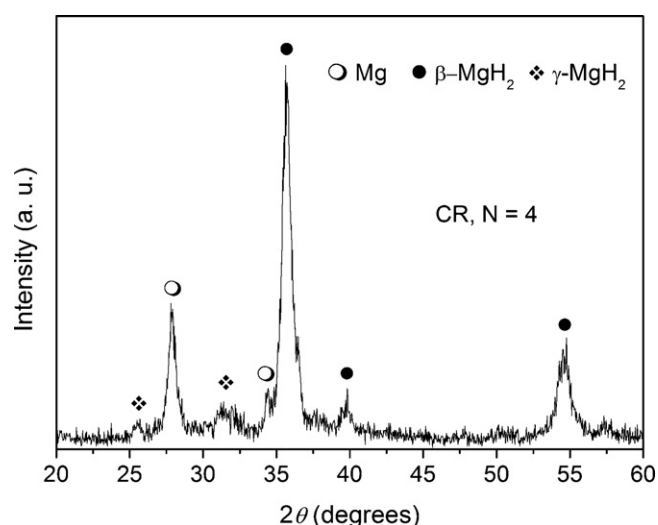


Fig. 2. XRD patterns of MgH_2 after 04 passes of CR.

system by the accumulation of structural defects, which allows the overcoming of the activation energy barrier to form the metastable phase [13]. In contrast, the metastable γ - MgH_2 was not detected in the samples processed by 5 passes of CF.

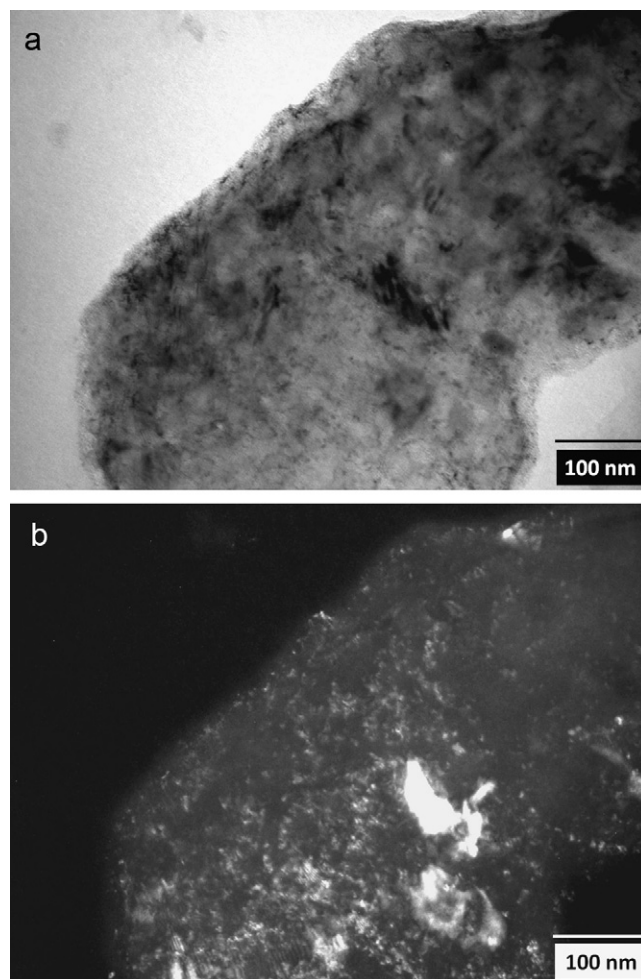


Fig. 3. (a) Bright field TEM image of MgH_2 after 04 passes of CR. (b) Corresponding dark field TEM image.

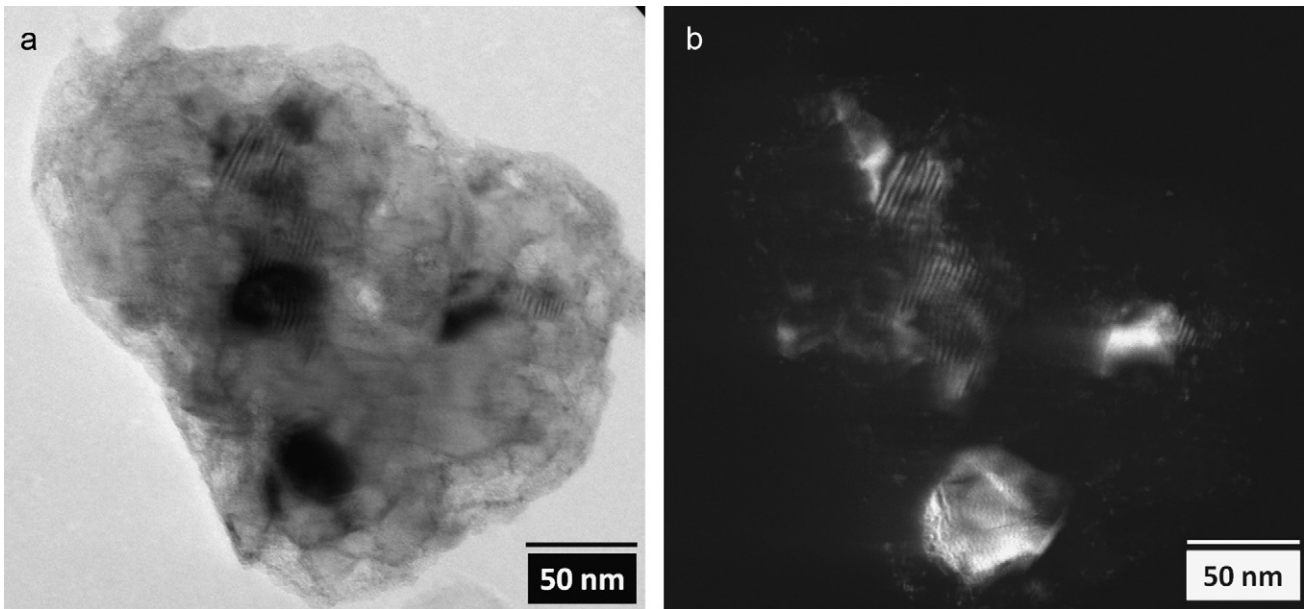


Fig. 4. (a) Bright field TEM image of MgH_2 after 5 passes of CF. (b) Corresponding dark field TEM image.

The MgH_2 samples processed by CR and CF presented preferred orientation, with an increase in the relative intensity of the peaks associated with the (1 0 1) planes. The same type of deformation texture is introduced in MgH_2 after HPT [11]. However, this texture is lost upon H-sorption cycling, as confirmed by XRD (not shown here).

In agreement with the differences concerning the formation of the metastable $\gamma\text{-MgH}_2$ phase, the processing by CR is more effective than CF in terms of refining the microstructure, at least with the conditions used here. The same crystallite size observed after

5 passes of CF was achieved in only 3 passes of CR and the level of texture developed after 5 passes of CF is basically the same as the one developed after only one pass of CR.

The tremendous level of grain refinement obtained after a few passes of CR and CF is comparable to the one attained typically after several hours of HEBM (for example, after 20 h in a SPEX mill [13]).

Fig. 3(a) shows a bright field TEM micrograph of MgH_2 after 04 passes of CR. Fig. 3(b) shows the dark field TEM image corresponding to the same areas showed in (a). It is clear in the micrographs

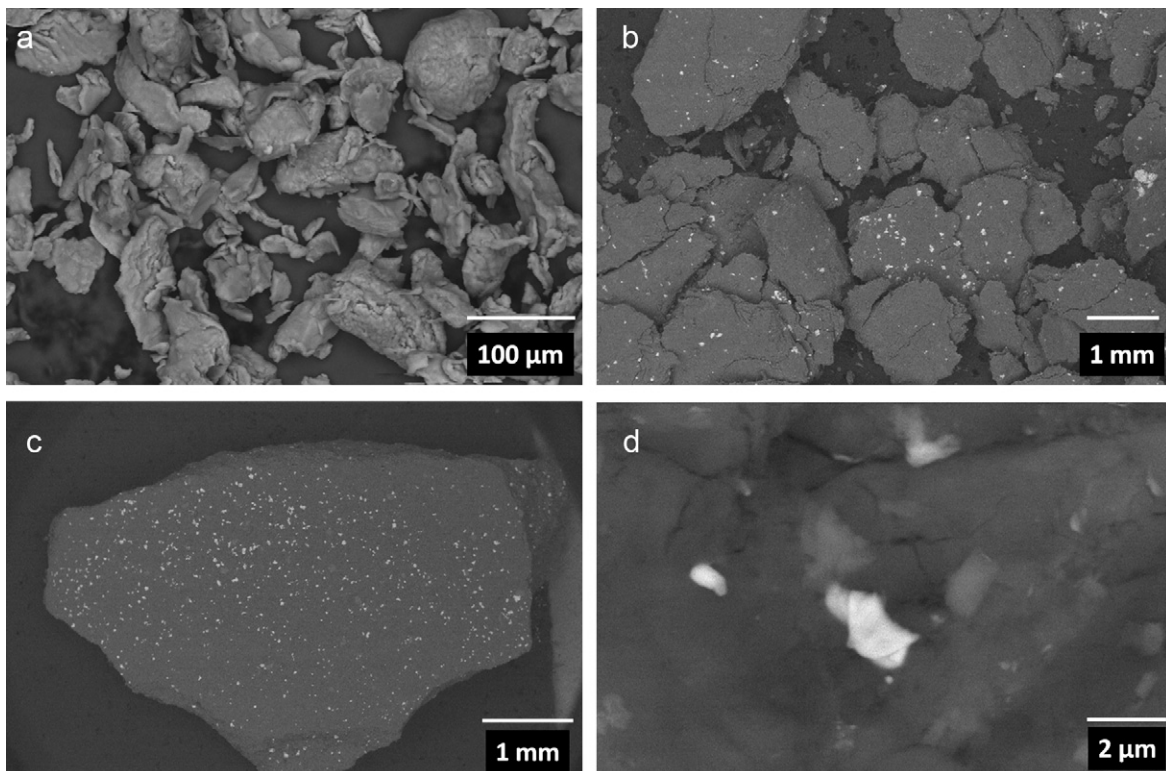


Fig. 5. BSE-SEM images of (a) MgH_2 and $\text{MgH}_2\text{-5\% Fe}$ after 04 passes of CR (b) and 05 passes of CF (c) and (d).

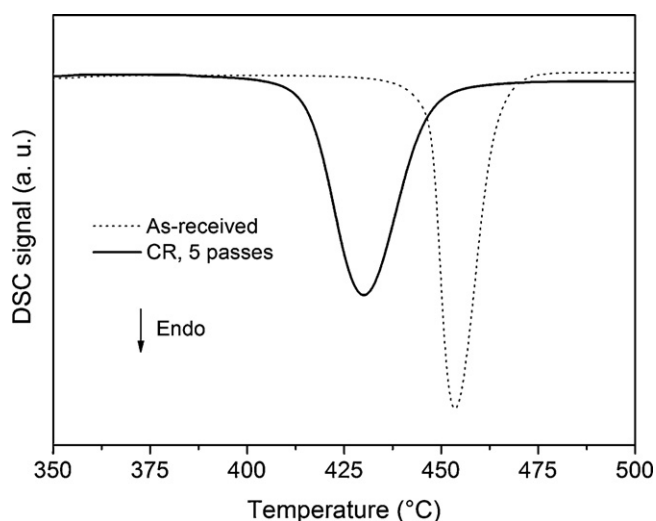


Fig. 6. DSC curve for the as-received MgH_2 and after 05 passes of CR.

the positive effect of the CR in terms of grain refining as already indicated by the XRD analyses.

Fig. 4(a) shows a bright field TEM image of MgH_2 after 5 passes of CF. The dark field TEM image shown in Fig. 4(b) confirms the small crystallite sizes deduced by the Scherrer analyses from the XRD patterns.

In addition to the small crystallites sizes observed in both CR and CF samples, the TEM images confirmed that there are differences in the deformation characteristics associated with each of these processes. In the CR sample, the crystallites are fragmented and agglomerated in a network which resembles a sub-grain structure. In the CF samples such networks have not been observed and individual nano-grains can be easily identified.

Fig. 5 shows backscattered (BSE) SEM images of the as received MgH_2 and also of the MgH_2 -5% Fe samples prepared by CR and CF. The powders have been consolidated during processing, forming small compacts, with diameters in the order of millimeters. A relatively good dispersion of Fe additive is obtained, despite of the low number of passes used. Although larger Fe particles are present in the mixture, there is a fraction of particles with diameters as low as $1\ \mu\text{m}$. A similar distribution of additives was also obtained for Mg -2.5% Pd alloys prepared by CR [14].

Fig. 6 shows DSC curves for the samples processed by CR in comparison with the as-received MgH_2 powder sample. Despite the large reduction in specific surface area as compared with the powder, an important decrease in the H-desorption temperature range is verified after CR, which can be certainly attributed to the nanoscale grain (or sub-grain) refinement after processing. This behaviour is contrary to the effect observed for nanocrystalline MgH_2 prepared by HEBM presenting different powder particle sizes [15].

Fig. 7 shows comparatively, H-sorption kinetics curves at $350\ ^\circ\text{C}$ for MgH_2 samples after CR and after CF and for MgH_2 + 5% Fe samples after CF. For all the samples absorption was carried out at 20 bar and desorption was carried out at 0.6 bar. The three types of samples show very good characteristics for hydrogen storage properties.

The hydrogen storage capacity is in the range of 5 wt.% for all the alloys with slightly better results for the CR sample. Desorption started faster in the CF MgH_2 -5% Fe sample but the total desorption time was basically the same as the CR MgH_2 sample. Absorption starts after the same time, a few minutes, for the three samples but, as already pointed out, final absorption capacity was better in the CR samples in comparison with CF samples.

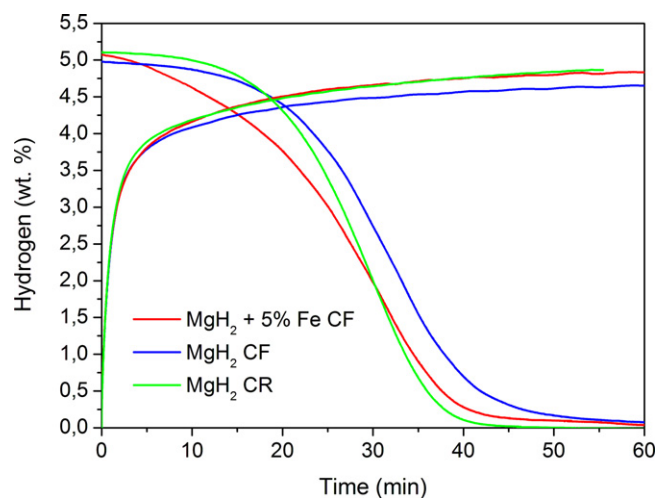


Fig. 7. H-sorption kinetics at $350\ ^\circ\text{C}$ of MgH_2 after CR, after CF and MgH_2 + 5% Fe after CF. Absorption at 20 bar and desorption at 0.6 bar.

Thus, the hydrogen storage properties seem to be better in CR samples, which presented a finer nano-structure than CF samples. Also important to report for comparison that commercial MgH_2 samples did not desorb at $350\ ^\circ\text{C}$ after many hours in the Sievert apparatus.

A final relevant aspect of our results is the much better air resistance of the bulk samples processed by CR in comparison with powder samples. Preliminary results indicate that samples stored many weeks in air still keeps very good hydrogen desorption properties, with only small differences in the temperatures of the DSC peaks. Such behaviour is of course, totally impossible to be obtained in conventional nano-structured powders, whose degradation begins immediately when in contact with air.

4. Conclusions

Mechanical processing of MgH_2 by cold rolling or cold forging leads to nanoscale grain refinement after only a few passes. Compared to HEBM, these procedures are much simpler, much less time and energy consuming and therefore show good potential for practical application.

Processing by cold work, both by CR or by CF, resulted in samples with the shape of small compacts with diameters in the order of millimeters. In the sample with Fe addition, CF also resulted in a good dispersion of the additives. These characteristics combined with the nanocrystalline structure of MgH_2 , results in attractive H-sorption kinetics and improved air-resistance when compared to MgH_2 nanocrystalline powder prepared by HEBM.

Acknowledgments

The authors would like to thank FAPESP, CNPq and CAPES for financial support.

References

- [1] G. Liang, J. Huot, S. Boily, A. Van Neste, R. Schulz, J. Alloys Compd. 292 (1999) 247–252.
- [2] W. Oelerich, T. Klassen, R. Bormann, J. Alloys Compd. 315 (2001) 237–242.
- [3] A.R. Yavari, A. LeMoulec, F.R. Castro, S. Deledda, O. Friedrichs, W.J. Botta, G. Vaughan, T. Klassen, A. Fernandez, A. Kvik, Scripta Mater. 52 (2005) 719–724.
- [4] B. Sakintuna, F. Lamari-Darkrim, M. Hirscher, Int. J. Hydrogen Energy 32 (2007) 1121–1140.
- [5] V. Skripnyuk, E. Rabkin, Y. Estrin, R. Lapovok, Acta Mater. 52 (2004) 405–414.
- [6] V. Skripnyuk, E. Buchman, E. Rabkin, Y. Estrin, M. Popov, S. Jorgensen, J. Alloys Compd. 436 (2007) 99–106.

- [7] S. Løken, J.K. Solberg, J.P. Maehlen, R.V. Denys, M.V. Lototsky, B.P. Tarasov, V.A. Yartys., *J. Alloys Compd.* 446–447 (2007) 114–120.
- [8] A. Wiczorek, M. Krystian, M.J. Zehetbauer, *Solid State Phenom.* 114 (2006) 177–182.
- [9] R.B. Figueiredo, T.G. Langdon, *Int. J. Mater. Res.* 100 (2009) 1638–1645.
- [10] D.R. Leiva, D. Fruchart, M. Bacia, G. Girard, N. Skryabina, A.C.S. Villela, S. Miraglia, D.S. Santos, W.J. Botta, *Int. J. Mater. Res.* 100 (2009) 1739–1747.
- [11] D.R. Leiva, A.M.Jr. Jorge, T.T. Ishikawa, J. Huot, D. Fruchart, S. Miraglia, C.S. Kiminami, W.J. Botta, *Adv. Eng. Mater.* 12 (2010) 786–792.
- [12] L. Lu, M.O. Lai, *Mechanical Alloying*, Kluwer, Boston, 1998.
- [13] J. Huot, G. Liang, S. Boily, A. Van Neste, R. Schulz, *J. Alloys Compd.* 293–295 (1999) 495–500.
- [14] J. Dufour, J. Huot, *J. Alloys Compd.* 439 (2007) L5–L7.
- [15] R.A. Varin, T. Czujko, Ch. Chiu, Z. Wronski, *J. Alloys Compd.* 424 (2006) 356–364.